Criticality Studies of a Nuclear Light Bulb Engine

THOMAS S. LATHAM*
United Aircraft Research Laboratories, East Hartford, Conn.

Determination of the feasibility of a nuclear light bulb engine is the subject of a continuing research program, and some of the results of this research are discussed in the article. Critical masses of U-233 fuel are calculated for a seven-cavity, nuclear light bulb engine in which energy is transferred by thermal radiation from gaseous nuclear fuel through internally cooled transparent walls to seeded hydrogen propellant. Each of the engine cavities is 6 ft long and 2.3 ft in diameter. BeO is employed between the unit cavities, and layers of BeO and graphite surround the seven units to provide neutron reflection. Effects of variations in the total moderator mass, the amount of BeO between unit cavities, the ratio of end wall to radial moderator mass, the amount of tungsten seed in the hydrogen propellant, and the amount of hafnium required to shield fuel injection and recirculation system ducts are evaluated analytically. The analysis also includes factors affecting the kinetic behavior of a nuclear light bulb engine: variations in fuel region radius, mixed mean propellant temperature, nominal system operating temperature, system operating pressure, and the proportion by weight of tungsten seen in the hydrogen propellant. For one specific nuclear light bulb engine, prompt neutron lifetime from two-dimensional neutron diffusion theory is calculated to be 0.52 msec, and comparable critical masses for U-233, U-235, and Pu-239 are 35, 50, and 46 lb, respectively, from one-dimensional neutron transport theory calculations.

Nomenclature

A_T	= effective area of nozzle throat, ft^2
$\overline{\cos\theta}$	= mean value of the cosine of the scattering angle for neutrons in the laboratory coordinate system
E	= neutron energy, ev
f_{IM}	= internal moderation fraction (see text)
f_{RM}	= radial moderator fraction, ratio of moderator mass in radial direction to total moderator mass
k_{eff}	= effective multiplication factor, dimensionless
M, M_c, M_{Hf}, M_W	= mass, critical mass, hafnium mass, and tungsten mass, respectively, lb
P_I/P_O	= ratio of power per unit cavity between inner and outer cavities
P_C	= nominal chamber operating pressure, atm
R_f	= fuel region radius, cm
T_{MM}	= mixed mean propellant temperature, °R
T_0	= nominal operating temperature, °R
v	= neutron velocity, cm/sec
$\Delta G/G_0$	= fractional change in parameter G from nominal value ($G = A_T, k, M, M_{Hf}$, etc.)
μ_{ij}	= probability for neutron energy transfer by scattering from neutron group i to j, dimensionless
σ_f	= microscopic fission cross section, barn
$\sigma_a{}^i, \sigma_s{}^i, \sigma_{tr}{}^i$	= microscopic absorption, scattering, and transport cross sections, respectively, for neutrons in energy group i, barn

Introduction

THE research discussed in this paper was conducted as part of a continuing investigation of the feasibility of the closed-cycle, vortex-stabilized, nuclear light bulb engine concept shown in Figs. 1 and 2. The engine employs seven separate, parallel cavities. In each cavity energy is transferred to seeded hydrogen propellant by thermal radiation from gaseous nuclear fuel suspended in a neon vortex.[1] The vortex and propellant regions are separated by an internally cooled transparent wall. Neon is injected to drive the vortex, passes axially toward the end walls, and is removed through a port at the center of one or both end walls. The resulting aerodynamic configuration is referred to as a "radial inflow" vortex. The neon discharging from the cavity, along with any entrained fuel and fission products, is cooled by being mixed with low-temperature neon, thus causing condensation of the nuclear fuel into liquid form. The liquid fuel is centrifugally separated from the neon and pumped back into the vortex region. The neon is then further cooled and pumped back to drive the vortex.

The primary objectives of the present investigations were 1) to evaluate the effects of possible variations in engine design (e.g., mass and distribution of moderator materials, exhaust nozzle throat area, and amounts of neutron poisons in propellant and moderator regions) on U-233 critical mass, 2) to evaluate factors affecting dynamics of a nuclear light

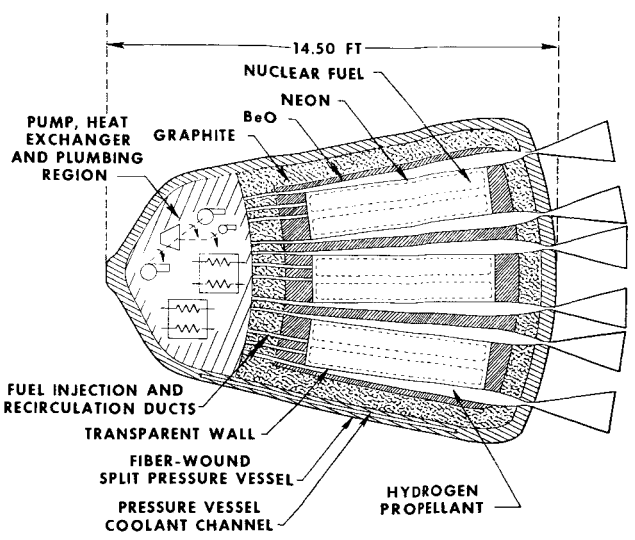

Fig. 1 Schematic diagram of reference nuclear light bulb engine.

Presented as Paper 68-571 at the AIAA 4th Propulsion Joint Specialist Conference, Cleveland, Ohio, June 10–14, 1968; submitted July 8, 1968; revision received June 2, 1969. Research supported by the joint AEC-NASA Space Nuclear Propulsion Office under Contract NASw-847.

* Senior Research Engineer.

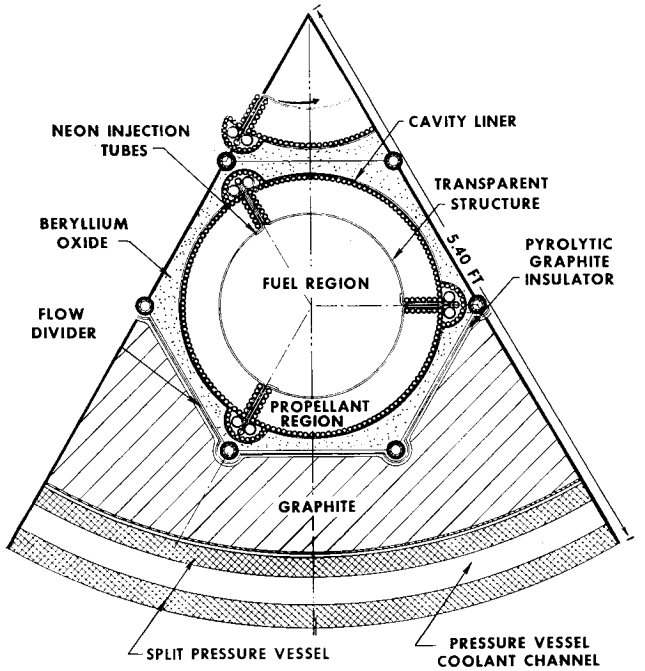

Fig. 2 60° sector or reference nuclear light bulb engine.

bulb engine such as prompt neutron lifetime, variations in nominal operating temperature and pressure and in fuel region radius, and fluctuations in fuel and propellant seed injection rates, and 3) to compare critical mass requirements using U-233 to those for U-235 and Pu-239 in a reference nuclear light bulb engine.

Engine Configuration

The reference engine (Figs. 1 and 2) has seven 2.3-ft-diam × 6-ft-long cavities or cells with moderator material located between the cavities and surrounding the assembly of cavities. The total volume of the 7 cavities is 169.8 ft^3 (equal to the volume of a single 2.3-ft-diam × 6-ft-long cavity). The total vortex volume is equal to half of the total cavity volume, or 84.9 ft^3. The cavity operating pressure is 500 atm. The radius of the fuel containment region is assumed to be 85% of the radius of the transparent wall. The fuel radiating temperature is assumed to be 15,000°R, and the propellant exit temperature is 80% of this value, or 12,000°R.

A fuel radiating temperature of 15,000°R produces a blackbody heat flux at the outside edge of the fuel containment region of 24,300 Btu/sec-ft^2, which, for the total surface area of the seven fuel containment regions (179.8 ft^2), produces a total power of 4.37 × 10^6 Btu/sec or 4600 Mw. The engine specific impulse is 1870 sec, and the total flow passing through the nozzle exit is 49.3 lb/sec, yielding a thrust of 92,000 lb. The engine size and radiating temperature chosen provide an engine power approximately equal to that considered for advanced solid-core nuclear rockets. Figure 2 is a cross-sectional view of a 60° sector of the engine showing details of one of the 6 peripheral cells and a sector of the central cell.

Approximately 15% of the total fission energy created is deposited by neutrons and gamma rays in the moderator materials and entrained in the neon recirculation system. The hydrogen propellant must remove this heat from the moderator materials plus the heat from the neon recirculation system. Therefore, the hydrogen's inlet enthalpy must be 15% of its exit enthalpy, or 15,500 Btu/lb, corresponding to a temperature of 4050°R. The hydrogen is seeded with ~4% by weight of tungsten particles to make it sufficiently opaque to allow only 2% of the radiated energy to reach the cavity walls.

The basic cylindrical geometry used for nuclear calculations is shown in Fig. 3. The compositions of the various regions and total weights of materials employed in the reference engine are given in Tables 1 and 2. The regions containing hot gases and the transparent walls contain hydrogen and neon at various temperatures to simulate relatively cool boundary layers adjacent to the transparent walls (SiO_2 at 2000°R and the cavity liner tubes at 1360°R). The cavity liner is made of internally cooled beryllium tubes coated with aluminum to provide high reflectivity for the incident thermal radiation. All of these materials, including the cavity liner, are homogenized into a single hot gas region for the nuclear calculations in order to conserve mesh points and computation time.

Additional regions that were homogenized to reduce computation time in two-dimensional calculations include the pump, heat exchanger, and plumbing region above the upper end walls, the upper and lower end walls, and the fiber-wound pressure vessel. Region 2 in Fig. 3 contains

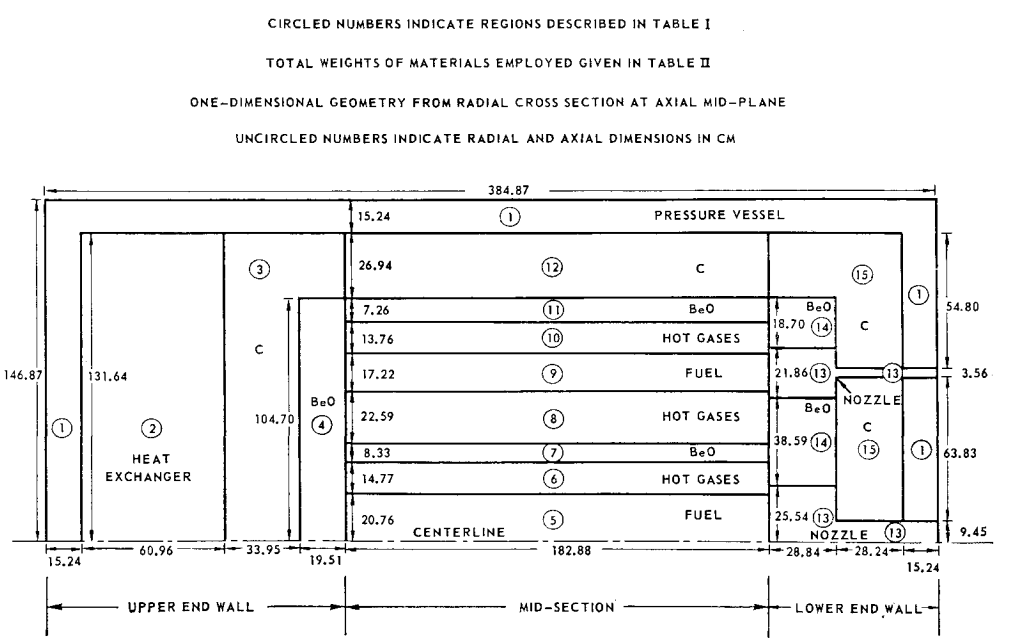

Fig. 3 Basic cylindrical geometry used for one- and two-dimensional criticality calculations.

Table 1 Compositions of regions in one- and two-dimensional calculations for reference engine (geometry and dimensions of regions shown in Fig. 3)

		Volume fractions													
	Region[a]	Ne 15,000[b]	Ne 2,000	SiO_2 2,000	H_2 2,000	H_2 12,000	H 12,000	H_2 4,000	Al 1,360	Be 1,000	BeO 2,529	C 4,086	Hf 1,000	SS 1,000	W-nat 4,000
6,8,10	Hot Gases	0.1327	0.0572	0.0289	0.2031	0.2500	0.2355	0.0789	0.0002	0.0134	...	...	...	...	...
7	Inner BeO	...	0.0073	0.0422	0.2192	...	...	...	...	0.0183	0.6918	0.0194	...	...	...
11	Outer BeO	...	0.0025	0.0190	0.1267	...	...	...	...	0.0640	0.7802	0.0066	...	...	...
4	Upper BeO	...	0.0061	0.0071	0.0980	...	...	0.1611	0.0005	0.0137	0.6953	0.0056	0.0035	...	...
14	Lower BeO	...	0.0022	0.0171	0.1140	...	...	...	...	0.0576	0.7022	0.0059	...	...	...
12	Outer graphite	...	...	...	...	...	...	0.0486	...	0.0011	...	0.9503	...	...	...
3	Upper graphite	...	0.0061	0.0071	0.0980	...	...	0.1611	0.0005	0.0137	...	0.6909	0.0035	...	...
15	Lower graphite	...	...	...	...	...	...	0.1437	...	0.0010	...	0.855ρ	...	...	...
13	Nozzles	...	...	...	...	0.5149	0.4851	...	...	...	...	...	...	...	...
1	Pressure vessel[c]	...	...	...	...	...	...	...	...	...	...	...	...	...	...
2	Heat exchanger	...	...	...	0.8700	...	...	...	...	...	...	...	...	0.1260	0.0040

[a] Fuel region volume fractions (regions 5,9) in a mixture of U-233 and Ne were varied to achieve criticality with the constraint that the sum of the U-233 and Ne atom densities was equal to 9.0×10^{19} atoms/cm^3.
[b] Numbers beneath elements are temperatures, °R.
[c] Pressure vessel composition was as follows: Volume fraction of fiberglass and resin = 0.80; volume fraction of internal hydrogen coolant (H_2 at 432 R, 250 atm) = 0.20; composition of fiberglass and resin laminate by weight [resin, $C_6H_4(NH_2)_2$ = 24.0%; SiO_2 = 49.4%; Al_2O_3 = 19.0%, MgO = 7.5%].

steel structure to help carry gravitational loads on the reactor core in addition to the pumps, heat exchangers, and piping containing propellant and coolant fluids. Unoccupied portions of region 2 are pressurized with hydrogen at 500 atm. The graphite and BeO upper end walls (regions 3 and 4 in Fig. 3, respectively) contain manifolds for coolant and propellant plus hafnium-shelded fuel injection and recirculation system ducts. Hafnium is employed to shield the fuel in the ducts from the high thermal neutron fluxes in these regions, thereby preventing excessive localized heating. The hafnium wall thicknesses were based on previously reported calculations.[2] The BeO and graphite lower end walls (regions 14 and 15 in Fig. 3) contain the same materials as the radial outer BeO and outer graphite (regions 11 and 12, respectively) with a 10% reduction in volume fraction of solid material to allow for plenums for collecting and turning moderator coolant flow.

In general, 5% of all moderator volume is devoted to small-diameter passages containing hydrogen coolant at 500 atm. Hydrogen is also present at 250 atm and at a volume fraction of 0.20 between two layers of the fiber-wound pressure vessel to provide internal cooling. The BeO associated with each unit cavity contains, in addition to hydrogen coolant passages, SiO_2 ducting for distribution and circulation of the cavity linear and transparent wall coolant, and internally cooled graphite-insulated beryllium tie rods. A flow divider and pyrolytic graphite insulating layer separates the outer hot graphite from the BeO associated with the unit cavities (Fig. 2).

Table 2 Densities and weights of materials employed in reference engine criticality calculations (see Fig. 3 and Table 1)

Material	Density, lb/ft^3	Total mass in all regions, lb
Neon: 15,000°R	0.94	14.8
Neon: 2,000°R	6.93	52.6
SiO_2: 2,000°R	157.3	890.0
Hydrogen: 12,000°R	0.075	16.0
Hydrogen: 4,000°R	0.34	14.6
Hydrogen: 2,000°R	0.69	99.7
Aluminum: 1,360°R	168.5	12.5
Beryllium: 1,000°R	114.8	764.0
BeO: 2,529°R	178.2	12200.0
Graphite: 4,068°R	114.8	26800.0
Hafnium: 1,000°R	823.7	131.6
Pressure vessel: 432°R	122.0	23400.0
Stainless steel: 1,000°R	500.4	7394.0
Tungsten: 4,068°R	1173.0	550.0
Hydrogen: 432°R	1.37	67.9
Total mass		72407.7

Nuclear Analysis and Cross Sections

The configuration shown in Fig. 3 contains adjacent zones with widely differing neutron scattering and absorption properties. Such a configuration requires a large number of mesh points for either neutron transport or diffusion theory calculations. In the interests of a reasonable computation time, one-dimensional calculations were performed using the ANISN neutron transport theory code,[3] for a geometry corresponding to a radial cross section through the midplane of Fig. 3. The minimum order of angular quadrature was chosen to be S4 (each quadrant divided into six weighted solid angles in cylindrical geometry) on the basis of previously calculated results.[4]

It was necessary to employ several thermal neutron energy groups in the range from 0 to 1.125 ev to calculate the neutron absorptions and spectra accurately for adjacent regions in the moderator at quite different temperatures. In addition, to calculate the effects of neutron up-scattering by the presence of hydrogen and hot neon in temperature ranges from 2000° to 12,000°R in the gaseous fuel regions, it was necessary to add several thermal neutron groups in the range between 1 and 29 ev. The basic set of 24 neutron energy groups was chosen with 14 of the groups covering the range from 0 to 29 ev and the remaining groups covering the range from 29 to 10^7 ev (Table 3).

In order to calculate two-dimensional configurations economically, the 24-group cross sections used in one-dimensional finite-cylinder calculations were used to generate volume- and flux-weighted 4-group cross section.[4,5] The neutron energy boundaries of the 4-group set are also shown in Table 3. The boundary between groups 3 and 4 in the 4-group set is at 8.32 ev, and some up-scattering of neutrons from group 4 to group 3 did occur. To eliminate up-scattering probabilities from the two-dimensional problems, the option in the ANISN code, which subtracts the up-scattering from the down-scattering and thereby maintains the balance of transfer of neutrons between adjacent groups, was used.[3] This created a 4-group cross section set that had only down-scattering.

Two-dimensional calculations were carried out using the 4-group cross sections in the EXTERMINATOR-II neutron diffusion theory code.[6] One two-dimensional transport theory calculation was carried out for the reference engine of Fig. 3 using S4 angular quadrature in the DOT code.[7] Mesh spacings and 4-group cross sections used for the two-dimensional neutron transport theory calculation were identical to those employed for the diffusion theory calculations so that an accurate comparison of results could be made. Eigenvalue convergence criteria were ≤ 0.0001 for all one-dimensional calculations and ≤ 0.0005 for all two-dimensional calculations.

Fast neutron cross sections were calculated using the GAM-I code with slowing-down spectra calculated for the various local moderator materials.[8] The slowing-down spectrum in the cavity regions was assumed to be that of the beryllium oxide moderator, the material in largest quantity adjacent to the cavities. Thermal neutron absorption cross sections were calculated using the TEMPEST code with spectra again chosen for the temperature and materials of the local moderator regions.[9] Up- and down-scattering probabilities within the thermal neutron energy groups were calculated using the SOPHIST-I code.[10] The SOPHIST-I code includes in the up- and down-scattering probabilities the enhancement of reaction rates due to relative velocity between neutron and scatterer; this effect was included in the calculation of the transport cross sections for the various materials.

Treatment of the transport cross section in the special cases of H and H_2 and hot Ne follows that reported in earlier calculations with the addition of dependence of the scattering cross section of H_2 on the energy of interaction, a function of relative velocity.[4,11] The equation for the transport cross section is

$$\sigma_{tr}{}^i = \sigma_a{}^i + \left(\sum_{j=1}^{13} \mu_{ij}\right) \sigma_s{}^i(1 - \overline{\cos\theta})^i \qquad (1)$$

The sum of μ_{ij} is the sum of the up- and down-scattering probabilities from energy group i to all energy groups j; $\overline{\cos\theta}$ is the mean value of the cosine of the scattering angle (which includes consideration of the motion of the scatter as well as the incident neutron); and $\sigma_s{}^i$ allows for the relative velocity dependence necessary to correct for the effects of molecular binding on the scattering cross section at low interaction energies.[11]

Effects of Variations in Engine Design

An objective of this study was to evaluate the effects of possible variations in reference engine design on the U-233 critical mass. Two-dimensional neutron diffusion theory calculations were performed in which the size and compositions of the gaseous regions remained the same but the total mass of moderator material was reduced. The ratio of BeO to graphite moderator weight was chosen for each of these configurations on the basis of simplified one-dimensional heat balance calculations in which it was assumed that neutron and gamma energy deposition was constant in the inner BeO regions and dropped off exponentially in the external BeO and graphite regions. The ratio of radial moderator mass to total moderator mass was assumed to be 0.5. The term radial moderator mass refers to all moderator mass between the upper and lower end walls in Fig. 3 (i.e., regions 7, 11, and 12). The remaining moderator material beyond the ends of the unit cavities is referred to as end-wall moderator mass (i.e., regions 3, 4, 14, and 15). The internal moderation factor f_{IM} was 0.143. This factor is the ratio of inner BeO mass (region 7 in Fig. 3) to the total BeO mass in the entire engine (regions 4, 7, 11, and 14). Normally, the inner BeO would contain all the BeO associated with the inner unit cavity and half of the BeO associated with the six outer cavities, in which case the internal moderation factor would be 0.286. An internal moderation factor of 0.143 means that half of the BeO that would normally be located in the inner BeO region has been shifted outward to the outer BeO region. It is shown later that changes in the BeO distribution can be made to minimize critical mass and, more importantly, to balance the rate of power output per unit cavity between the inner and outer cavities.

Table 3 Neutron energy group structures used in criticality calculations

Neutron energy group	Upper energy limit, ev	Lower energy limit, ev	Group 4-group number for structure
1	1.0×10^7	2.865×10^6	
2	2.865×10^6	1.35×10^6	1
3	1.35×10^6	8.21×10^5	
4	8.21×10^5	3.88×10^5	
5	3.88×10^5	1.11×10^5	
6	1.11×10^5	1.50×10^4	2
7	1.50×10^4	3.35×10^3	
8	3.35×10^3	5.83×10^2	
9	5.83×10^2	1.01×10^2	3
10	1.01×10^2	29.0	
11	29.0	8.32	
12	8.32	3.06	
13	3.06	2.38	
14	2.38	1.86	
15	1.86	1.44	
16	1.44	1.125	
17	1.125	0.685	
18	0.685	0.414	4
19	0.414	0.3	
20	0.3	0.2	
21	0.2	0.1	
22	0.1	0.05	
23	0.05	0.015	
24	0.015	0.0	

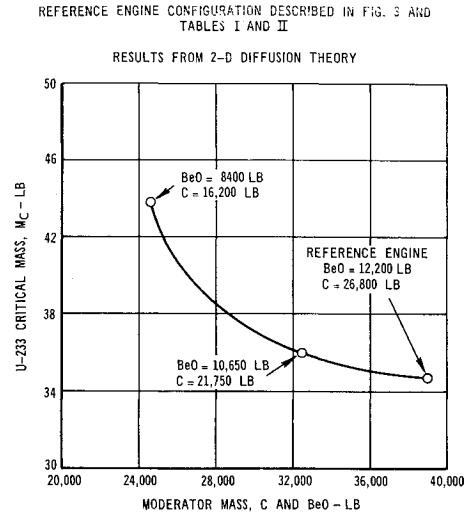

Fig. 4 Effect of variation of total moderator mass on U-233 critical mass.

Figure 4 shows that a decrease in total moderator mass from 39,000 to 24,600 lb results in an increase in U-233 critical mass M_c from 34.7 to 43.8 lb. In comparison, the total moderator mass in the configuration employed in Ref. 4 was 33,100 lb, and M_c was 43.5 lb.

One-dimensional, 4-group transport theory calculations were performed to investigate the effect of the amount of internal moderation. An effective cylinder height was chosen such that the critical fuel loading matched that from the earlier two-dimensional result, and f_{IM} was varied between 0 and 0.286 and M_c was minimum at $f_{IM} = 0.190$ (Fig. 5). The reference engine was chosen to have a value of f_{IM} of 0.143 because the ratio of power per unit cavity between the inner and outer cavities would be closer to unity with relatively little increase in critical mass. This ratio P_I/P_O is also shown in Fig. 5 with one point of comparison for the reference engine from the two-dimensional diffusion theory results. Further reduction in P_I/P_O from 1.14 to 1.0 would have to be achieved by different fuel loadings in the

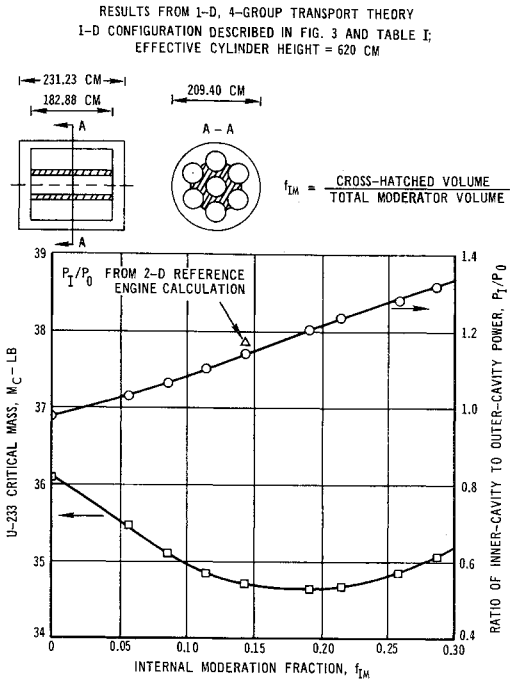

Fig. 5 Effect of internal moderation on U-233 critical mass and ratio of inner-cavity to outer-cavity power.

inner and outer cavities. The reduction in M_c from $f_{IM} = 0$ to the minimum point at $f_{IM} = 0.190$ was ~5%.

Another factor affecting M_c is the distribution of moderator mass between radial and axial directions. Two-dimensional diffusion theory calculations showed (Fig. 6) that M_c is minimized when the fraction of total moderator mass used in the radial direction f_{RM} is 0.5. Figure 7 shows results of two-dimensional diffusion theory calculations in which the effective nozzle throat area A_T was varied. [Note that $(\Delta M/M_c)/(\Delta A_T/A_{T_0}) = +0.156$ at the reference engine design point.] At the point where $A_T = 0$, only the nozzle throat was closed off, with the nozzle approach still in the BeO portion of the lower end wall (region 14 in Fig. 3). The

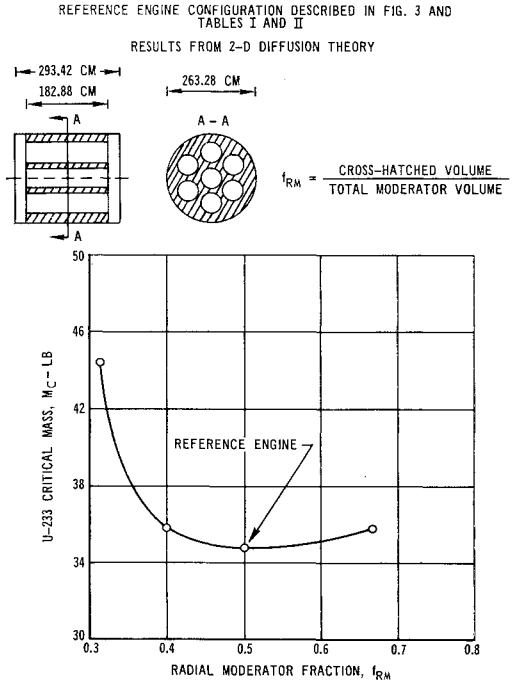

Fig. 6 Effect of variation of the ratio of radial-to-total moderator mass on U-233 critical mass.

nozzle approach and throat areas of the reference engine were calculated on the basis of splitting the nozzle volume between the lower BeO, the lower graphite, and the pressure vessel regions with the assumption that the nozzle radius varied linearly with distance from the base of the unit cell to the outside edge of the pressure vessel. The actual nozzle throat area per unit cell was 0.006 ft², as reported in Ref. 1. The relatively large A_T of 2.1 ft² employed in the reference engine calculations was chosen to allow for the effects of structure and coolant manifolds around the nozzle throats. For the reference engine, M_c = 34.7 lb, which corresponds to an average fuel partial pressure in the fuel-containment region of 200 atm on the basis of radiation heat-transfer studies.[12]

Material worths were calculated using the EXTERMINATOR-II adjoint and perturbation calculation options. Table 4 presents the resulting reactivity coefficients, which were used to estimate the effects on M_c to be expected 1) from seeding the H_2 with 4% W, and 2) from reduction in the size of the Hf-shielded fuel injection and recirculation system ducts in the upper end walls. Tungsten seed was included in the two-dimensional diffusion theory calculations in only trace amounts in the nozzle regions and in the hydrogen. Applying the reactivity coefficients of Table 4 to the inclusion of 4% W by weight in the hydrogen would decrease k_{eff} by 0.001, which would result in an increase in M_c of 0.09 lb.

The major portion of the hafnium in the upper end walls is due to fuel recirculation system ducts that were assumed to require twelve times the flow area of the fuel injection ducts to accommodate the neon bypass flow required to cool the recirculating fuel. If this flow area were halved, the required hafnium mass in the end wall would be reduced by about 30%, k_{eff} would increase by 0.004, and M_c would decrease by 0.36 lb. The hafnium duct walls in the upper end wall were assumed to be 0.2 in. thick, and the hafnium cross sections employed in all calculations had self-shielding factors applied to them.[13]

Factors Affecting Dynamics of a Nuclear Light Bulb Engine

Some of the factors that can affect the reactivity of any type of gaseous nuclear rocket engine have been investigated using the EXTERMINATOR-II adjoint-perturbation calculations and one-dimensional 24-group transport theory calculations for the reference nuclear light bulb engine.

The reference engine has different nominal operating temperatures T_0 in different regions as shown in Tables 1 and 2. These temperatures were varied by ±20%. In gaseous regions, pressure was assumed to remain constant at 500 atm, and an effective cylinder height of 620 cm was used. Figure 8 shows that there is a positive temperature coefficient of reactivity at T_0 (+0.0450, Table 4), with the slope falling

Table 4 Table of reactivity coefficients for reference engine

Material or region	Reactivity coefficient	
U-233	$(\Delta k/k)/(\Delta M/M_c)$	$= +0.3840$
Neon and hydrogen, all regions	$(\Delta k/k)/(\Delta P_C/P_{C_0})$	$= +0.0859$
All regions	$(\Delta k/k)/(\Delta T/T_0)$	$= +0.0450$
Hydrogen gases in propellant region	$(\Delta k/k)/(\Delta T_{MM}/T_{MM_0})$	$= +0.0544$
Fuel region	$(\Delta k/k)/(\Delta R_f/R_{f_0})$	$= -0.0413$
Hafnium in upper end walls	$(\Delta k/k)/(\Delta M_{Hf}/M_{Hf_0})$	$= -0.01346$
Tungsten in propellant gases	$(\Delta k/k)/(\Delta M_W/M_{W_0})$	$= -2.31 \times 10^{-5}$
Tungsten in nozzle gases	$(\Delta k/k)/(\Delta M_W/M_{W_0})$	$= -6.30 \times 10^{-7}$

off at 1.2 T_0. The reason for the positive temperature reactivity coefficient can be seen by comparing the curve of average fission cross section for group 4 with the curve showing a $1/v$ variation. It should be emphasized that changes in density that occur as a result of a variation of temperature of the hot gases at constant pressure cause axial leakage variations that cannot be accurately accounted for in a one-dimensional calculation. Eventually, the effects of increased axial leakage must overcome the positive reactivity contribution due to the non-$1/v$ nature of the U-233 fission cross section. Evaluation of the temperature at which the slope of the temperature coefficient of reactivity changes sign should be the subject of further two-dimensional calculations.

The hydrogen propellant regions of the reference engine contain relatively cool boundary layers near the cavity walls and transparent walls. The thickness of these layers affect the mixed mean temperature T_{MM} of the propellant. Calculations using the one-dimensional transport theory model showed that $(\Delta k/k)/(\Delta T_{MM}/T_{MM_0}) = +0.0544$ resulted (Table 4) for variation of the T_{MM} about a basic value of $T_{MM_0} = 5100°R$. This positive reactivity coefficient is explained by the non-$1/v$ behavior of the group 4 fission cross section as previously discussed.

One-dimensional transport theory calculations also were done to determine the effect of fuel region radius variation for the reference engine configuration using an infinite cylinder height to eliminate possible variations in simulated axial leakages with the changes in fuel density resulting from changes in fuel volume. Total and local pressure in the chamber and nuclear fuel mass were held constant as fuel region radius R_f was changed. For the range of fuel-to-cavity radius ratio of 0.5 to 0.61, $(\Delta k/k)/(\Delta R_f/R_{f_0})$ was -0.0413 (Table 4). This result is contrary to what should be expected on the basis of self-shielding arguments. However, the self-shielding is so slight that it is overridden by the change in the non-$1/v$, U-233 average fission cross section caused when thermal neutrons traverse the layer of neon at 15,000°R, which increases in thickness as the fuel cloud is reduced in size. The calculations of R_f effects should be expanded to include two-dimensional R-θ calculations to determine whether a more accurate geometric description of the reference engine geometry in the cross-sectional plane has a significant effect on the results. In addition, R_f effects should be evaluated for cases in which compression and expansion of the fuel cloud occur so rapidly that local pressures do not remain constant, but vary in proportion to local fuel density.

The reactivity coefficients resulting from changes in the amount of tungsten seed in the hydrogen and changes in the amount of hafnium in the upper end walls have been discussed previously and are also shown in Table 4. The reactivity coefficient associated with all gases in all regions, obtained from the results of the two-dimensional adjoint-perturbation calculations, is also shown in Table 4. This reactivity coefficient can be interpreted as the pressure coefficient of reactivity and has a positive value of $(\Delta k/k)/(\Delta P_c/P_{c_0}) = +0.0859$. Prompt neutron lifetime was calculated for U-233 in the reference engine using the EXTERMINATOR-II adjoint-perturbation calculation; it was 0.516 msec.

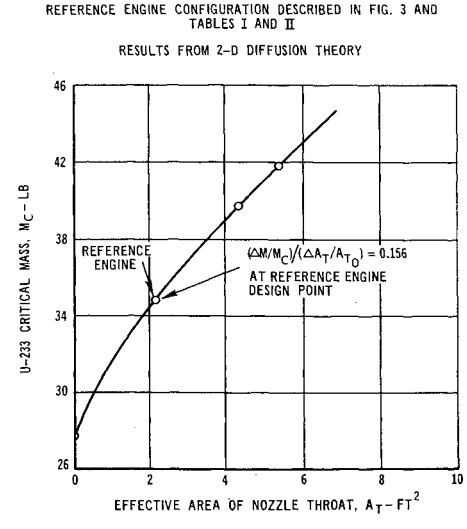

Fig. 7 Effect of variation of effective nozzle throat area on U-233 critical mass.

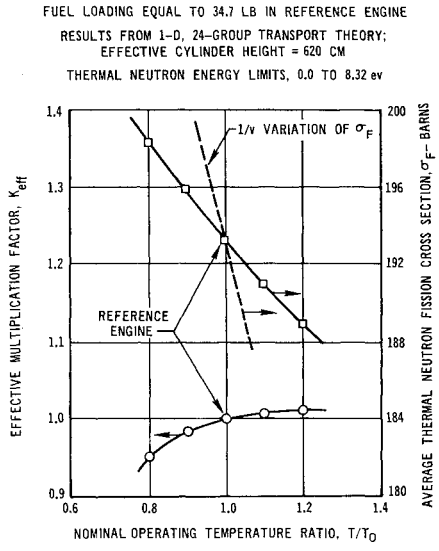

Fig. 8 Effect of variation in nominal operating temperature on effective multiplication factor and average thermal fission cross section.

Comparisons of Nuclear Fuels and Analytical Techniques

Two special one-dimensional, 24-group, neutron transport theory calculations were performed using the effective cylinder height of 620 cm to determine the required critical masses of Pu-239 and U-235 in the reference engine configuration. The results gave critical masses of 46.0 lb for Pu-239 and 50.4 lb for U-235. The corresponding M_c for U-233 was 34.7 lb. The higher M_c for U-235 compared with U-233 is due to both a lower average thermal fission cross section and a lower yield of neutrons per fission. In the case of Pu-239, the fission/absorption resonance at 0.3 ev gives rise to a substantially higher thermal neutron fission cross section but also a larger capture to fission ratio. Most important, the resonance cross sections become self-shielded, causing the M_c to be substantially higher than that required for U-233.

For purposes of comparison, one two-dimensional neutron transport theory calculation using the DOT code was performed using 4-group cross sections and mesh spacings identical to those used in the two-dimensional diffusion theory calculations for the reference engine. The results from transport theory yielded a critical mass of U-233 of 30.90 lb, which is 11% lower than that from diffusion theory. This M_c corresponds to an average fuel partial pressure of 175 atm in the fuel-containment region on the basis of radiation heat-transfer studies.[12] The transport theory result had about half as much total neutron leakage from the system as was calculated by diffusion theory, and the radial neutron flux plots differed somewhat in the outer BeO and graphite regions. This can be seen in Fig. 9, where comparisons of the normalized radial neutron fluxes from one- and two-dimensional transport theory and two-dimensional diffusion theory are presented.

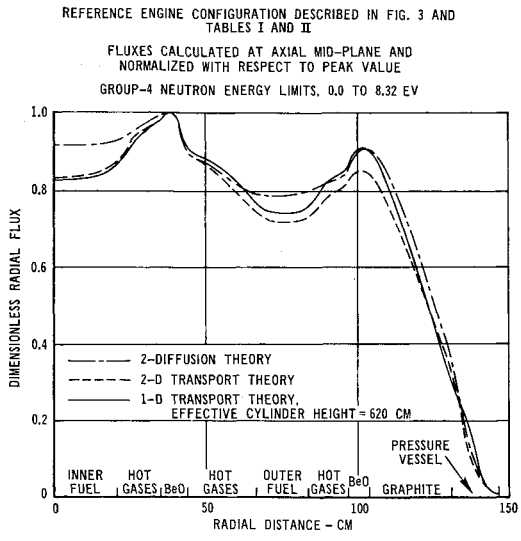

Fig. 9 Comparison of radial flux plots for one- and two-dimensional neutron diffusion and transport theory calculations.

Summary of Results

The following results were determined on the basis of two-dimensional neutron diffusion theory calculations. 1) A U-233 critical mass of 34.7 lb was determined for the reference engine, corresponding to an average fuel partial pressure in the fuel-containment region of 200 atm. 2) The optimum fraction of radial moderator to total moderator mass was 0.5; this resulted in minimum critical mass M_c for the reference engine. 3) The U-233 critical mass increased essentially linearly with increase in effective nozzle throat area for the reference engine; the ratio of fractional changes was $(\Delta M/M_c)/(\Delta A_T/A_{T0}) = +0.156$. 4) Inclusion of tungsten seed at 4% by weight in the hydrogen propellant increased M_c by only 0.09 lb. In the vicinity of this value, a negative reactivity coefficient resulted from an increase in the amount of tungsten seed. 5) A 30% reduction of hafnium in the upper end walls decreased M_c by only 0.36 lb. 6) A positive reactivity coefficient resulted from an increase in nominal operating pressure. 7) The calculated prompt neutron lifetime was 0.516 msec.

The following results were determined on the basis of one-dimensional neutron transport theory calculations. 1) The optimum internal moderation fraction was 0.19, but due to considerations of flattening power density, an internal moderation fraction of 0.14 was chosen for the reference engine. 2) Positive reactivity coefficients resulted from increases in nominal operating temperature and mixed-mean propellant temperature. 3) A negative reactivity coefficient resulted from an increase in fuel radius when the fuel cloud radius was changed, while chamber pressure and U-233 mass remained constant. 4) Critical masses using U-235 and Pu-239 in the reference engine were 50.4 and 46.0 lb, respectively, compared with 34.7 lb for U-233.

The following result was determined on the basis of two-dimensional neutron transport theory calculations: A U-288 critical mass of 30.9 lb was determined for the reference engine, which is 11.0% less than that calculated using two-dimensional diffusion theory. This compares to a U-233 critical mass of 43.5 lb for an earlier reference engine with substantially greater amounts of neutron-absorbing structural materials in the end walls and nozzle approach regions. The critical mass of 30.9 lb corresponds to an average fuel partial pressure of 175 atm in the fuel-containment region.

References

[1] McLafferty, G. H. and Bauer, H. E., "Studies of Specific Nuclear Light Bulb and Open-Cycle Gaseous Nuclear Rocket Engines," Rept. F-910093-37, Contract NASw-847, Sept. 1967, United Aircraft Research Lab.; also CR-1030, NASA.

[2] Latham, T. S., "Heat Generation in Nuclear Fuel During Injection into a Gaseous Nuclear Rocket Engine," AIAA Paper 66-620, Colorado Springs, Colo., 1966.

[3] Engle, W. W., "A Users Manual for ANISN, A One-Dimensional Discrete Ordinates Transport Code With Anisotropic Scattering," Rept. K-1693, March 30, 1967, Nuclear Div., Union Carbide Corp.

[4] Latham, T. S., "Nuclear Criticality Studies of Specific Nuclear Light Bulb and Open-Cycle Gaseous Nuclear Rocket Engines," Rept. F-910375-2, Contract NASw-847, Sept. 1967, United Aircraft Research Lab.

[5] "Gaseous-Fueled Cavity Reactors, Criticality Calculations and Analysis," NASA CR-487, July 1966, General Motors Corp.

[6] Fowler, T. B., Tobias, M. L., and Vondy, D. R., "EXTERMINATOR-II: A Fortran IV Code For Solving Multigroup Neutron Diffusion Equations in Two-Dimensions," Rept. ORNL-4078, April 1967, Oak Ridge National Lab.

[7] Mynatt, F. R., "A Users Manual for DOT, A Two-Dimensional Discrete Ordinates Transport Code With Anisotropic Scattering," Rept. K-1964, Nuclear Div., Union Carbide Corp.

[8] Joanou, G. D. and Dudek, J. S., "GAM-1, A Consistent P-1 Multigroup Code for the Calculation of Fast Neutron Spectra and Multigroup Constants," Rept. GA-1850, June 1961, General Atomics.

[9] Shudde, R. H. and Dyer, J., "TEMPEST, A Neutron Thermalization Code," Sept. 1960, North American Aviation.

[10] Canfield, E. H. et al., "SOPHIST-I, An IBM 709/7090 Code which Calculates Multigroup Transfer Coefficients for Gaseous Moderators," Rept. UCRL-5956, Oct. 1961, Lawrence Radiation Lab., Univ. of California, Livermore, Calif.

[11] Latham, T. S., "Nuclear Criticality Study of a Specific Vortex-Stabilized Gaseous Nuclear Rocket Engine," Rept. E-910375-1, Oct. 1966, United Aircraft Research Lab.; also CR-697, NASA.

[12] Kesten, A. S. and Krascella, N. L., "Theoretical Investigation of Radiant Heat Transfer in the Fuel Region of a Gaseous Nuclear Rocket Engine," Rept. E-910092-9, Contract NASw-847, Sept. 1966, United Aircraft Research Lab.; also CR-695, NASA.

[13] Stewart, J. C. and Zweifel, P. F., *Proceedings of the Second International Conference on the Peaceful Uses of Atomic Energy*, Vol. 16, United Nations, New York, 1958, p. 650.